Dynamic equivalence between soft- and hard-core Brownian fluids

F. de J. Guevara-Rodríguez* and Magdaleno Medina-Noyola†
Instituto Mexicano del Petróleo, Programa de Ingeniería Molecular, Eje Central Lázaro Cárdenas 152, 07730 México, Distrito Federal, Mexico

(Received 18 December 2002; published 21 July 2003)

In this work, we demonstrate the dynamic equivalence between the members of the family of Brownian fluids whose particles interact through strongly repulsive radially symmetric soft-core potentials. We specifically consider pair potentials proportional to inverse powers of (r/σ). This equivalence is the dynamic extension of the static equivalence between all these pair potentials and the hard-sphere fluid, assumed in the treatment of soft-core reference potentials in the classical (Weeks-Chandler-Andersen or Barker-Henderson) perturbation theories of simple liquids. In contrast with the strict hard-sphere Brownian system, in the case of soft-sphere potentials the conventional Brownian dynamics algorithm is indeed well defined. We find that, except for small values of ν, and/or very short times, the dynamic properties of all these systems collapse into a single universal curve, upon a well-defined rescaling of the time and distance variables. This family of systems includes the hard-sphere limit. This observation permits a conceptually simple, new, and accurate Brownian dynamics algorithm to simulate the dynamic properties of the hard-sphere model dispersion without hydrodynamic interactions. Such an algorithm consists of the straightforward rescaling of the Brownian-dynamics simulated properties of any of the dynamically equivalent soft-sphere systems.

DOI: 10.1103/PhysRevE.68.011405 PACS number(s): 82.70.−y, 05.40.−a, 61.20.−p, 02.70.−c

I. INTRODUCTION

The hard-sphere (HS) fluid has played an outstanding role in the development of our fundamental understanding of simple liquids [1], and more recently, of concentrated colloidal dispersions [2]. The simplicity of this idealized interaction potential has allowed the proposal of extremely simple analytic expressions for some of its most relevant thermodynamic and structural equilibrium properties [1]. In other contexts, however, the very discontinuous nature of the HS pair potential turns out to be the source of considerable difficulties. In colloid dynamics, for example, the first cumulants of the intermediate scattering function $F(k,t)$ may be readily accessible by dynamic light scattering experiments, and can easily be calculated for continuous pair potentials [1–3]. For the HS system, in contrast, these short-time properties do not exist, since in this case $F(k,t)$ is not an analytic function of time. The short-time moments, and all the other relevant dynamic properties of model colloidal dispersions in equilibrium (and in the absence of hydrodynamic interactions), may also be simulated rather easily by the conventional Brownian dynamics (BD) algorithm of Ermak and McCammon [4,5] if the interparticle effective interactions can be described by continuous pair potentials. Also, due to the discontinuous nature of the HS interaction, however, this well-established algorithm, which relies on the calculation of particle-particle forces to describe Brownian collisions, becomes undefined for the HS system.

Several attempts to circumvent the latter difficulty have been reported in the literature. Some are based on an artificial definition of the collisions between Brownian hard spheres [6,7]. Others artificially avoid hard-sphere overlaps [8–15], which are inevitable in a straightforward application of the Brownian dynamics algorithm to a HS system involving a finite time step Δt. By means of a careful extrapolation procedure to the limit $\Delta t \to 0$, however, Cichocki and coworkers [8–11] were able to compute some of the dynamic properties of the equilibrium HS suspension in the absence of hydrodynamic interactions. Heyes and Brańka [16,17], on the other hand, have approached the Brownian dynamics simulation of these systems by considering repulsive soft-sphere potentials of the form $(\sigma/r)^{\nu}$ (whose $\nu \to \infty$ limit is the HS potential) for a sufficiently large, but finite, exponent ν; the BD algorithm is well defined for these potentials when ν remains finite. One interesting side result of the present work is a different approach to simulate the dynamics of the HS model suspension without hydrodynamic interactions. Such an algorithm is in some sense similar and complementary to that of Heyes and Brańka, although it is based on the application of a principle of dynamic equivalence between Brownian soft- and hard-sphere systems, whose discussion is the main subject of the present paper.

It is well known (see Sec. 6.3 of Ref. [1] for a textbook presentation) that the static structural properties of a repulsive soft-sphere system can be mapped, upon the definition of some effective diameter, onto the corresponding properties of a hard-sphere system. This means that the radial distribution function $g(r)$ of the soft-sphere system is approximately identical to that of an appropriately chosen HS system, except for a small region near $r=\sigma$ (or, without exception, if we describe the static structure in terms of the function $y(r)=\exp[\beta u_s(r)]g(r)$; see Ref. [18] and Fig. 1). Conversely, the static structure of the HS system at a given volume fraction can be represented by the structure of any of the soft-sphere systems in this family, up to some well-defined res-

*Electronic address: fguevara@imp.mx
†Permanent address: Instituto de Física "*Manuel Sandoval Vallarta*," Universidad Autónoma de San Luis Potosí, Álvaro Obregón 64, 78000 San Luis Potosí, San Luis Potosí, Mexico. Electronic address: medina@ifisica.uaslp.mx

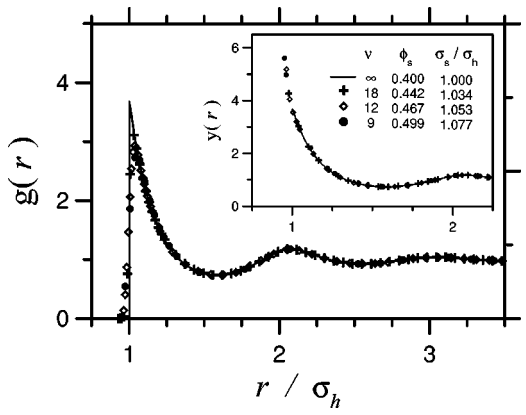

FIG. 1. Radial distribution function of three equivalent systems of soft spheres. The solid curve corresponds to the system of hard spheres with volume fraction of 0.4.

caling of the distance. This is equivalent to some form of the principle of equivalence or universality of the structural properties of all the systems in this family, and well-established prescriptions exist to determine the correspondence between any soft-sphere and its corresponding hard-sphere system [1]. For example, in approximating the properties of the reference system (repulsive soft-core potential) by those of the hard-sphere fluid, the well-known Weeks-Chandler-Andersen [19] (WCA) and Barker-Henderson [20] (BH) perturbation theories of liquids involve the use of this principle. Furthermore, they provide simple procedures to quantitatively establish such correspondence (e.g., the ''blip-function'' method [1] in the WCA theory). Thus, it is natural to question whether this static universality extends over to dynamic properties such as $F(k,t)$. Answering this question is the main purpose of this work.

Surprisingly enough, to the best of our knowledge, this expectation of dynamic equivalence has never been tested in detail. In this paper, we demonstrate that, at least in the context of the equilibrium dynamic properties of the family of model Brownian fluids considered here, this expectation indeed happens to be correct. As an interesting side product, this dynamic equivalence is employed to propose a different BD algorithm for hard-sphere suspensions without hydrodynamic interactions, which allows us to determine the dynamic properties of this system by means of a simple rescaling of the time and space variables of the simulated properties of any of the dynamically equivalent soft-sphere systems. As an illustration, we present some results for the Van Hove function and/or its Fourier transform $F(k,T)$ of the HS system, and compare them with the results of other authors.

In the following section, we recall the physical principle of static equivalence between soft- and hard-sphere systems. In Sec. III, we explain in detail the dynamic extension of this equivalence principle. Section IV describes the resulting Brownian dynamics algorithm for hard-sphere dispersions in the absence of hydrodynamic interactions. In Sec. V, we illustrate its application and discuss its limitations. Summary is contained in Sec. VI.

II. STATIC EQUIVALENCE BETWEEN SOFT AND HARD SPHERES

Consider a soft-sphere system consisting of N particles in a volume V, interacting through some form of soft repulsive but short-ranged pair potential $u_s(r)$. For our purpose, the particular form of this potential is irrelevant. For concreteness, however, we choose to write it, in units of the thermal energy $k_BT=\beta^{-1}$, as

$$\beta u_s(r)=\left(\frac{\sigma_s}{r}\right)^{2\nu}-2\left(\frac{\sigma_s}{r}\right)^{\nu}+1, \tag{1}$$

for $0<r\leqslant\sigma_s$, and such that it vanishes for $r>\sigma_s$. The only convenience of this particular functional form is that the potential and its derivative strictly vanish at, and beyond, σ_s. It is also the natural reference potential in the WCA perturbation theory for the $2\nu-\nu$ family of repulsive plus attractive interactions, which includes the Lennard-Jones potential ($\nu=6$). This, however, is not relevant in the present context.

Let us now imagine a hard-sphere system [i.e., the $\nu\to\infty$ limit of Eq. (1)] at exactly the same number concentration $n=N/V$. It has been long documented [1] that one can find a particular value for the hard-sphere diameter σ_h of this system, such that the structure of both systems would be virtually indistinguishable. In both, the WCA and the BH perturbation theories of liquids, prescriptions are given to determine the value of σ_h, for a given soft-potential (i.e., given ν and σ_s) and a given number density n. For example, the simplest of them is the so-called ''blip-function'' method, which adjusts σ_h such that the volume integral of the blip function, $[\exp[-\beta u_s(r)]-\exp[-\beta u_h(r)]]$, vanishes; other more accurate prescriptions can be consulted in the literature [1].

Exactly this correspondence between soft- and hard-sphere systems can be used in an inverse manner. Thus, for a given hard-sphere system (i.e., given number concentration n and HS diameter σ_h), one can determine the ''diameter'' σ_s of any soft-sphere system of the family described by the interaction potential in Eq. (1), whose structure, at the same concentration n, matches that of the given HS system. This implies that all the soft-sphere systems in the family in Eq. (1) are structurally identical to each other, in the sense that they share the same function $y(r)$, and hence, the structure of any member of this family can be used to represent the structure of any other, including, of course, the HS system itself.

What we mean for ''structurally identical'' is quantitatively illustrated in Fig. 1. There, the radial distribution function (rdf) $g(r)$ of three soft-sphere systems ($\nu=9$, 12, and 18, simulated by the conventional Brownian dynamics algorithm [4,5]) are plotted, along with the rdf of the hard-sphere system at a volume fraction $\phi_h\equiv\pi n\sigma_h^3/6=0.4$ (simulated with the conventional Monte Carlo algorithm [5]). Note that various rdfs differ near $r=\sigma_h$ because of the factor $\exp[-\beta u_s(r)]$ in $g(r)=\exp[-\beta u_s(r)]y(r)$. Hence, the structural equivalence is most dramatically exhibited by the universality of the function $y(r)$, as illustrated in the inset of Fig. 1. Also note that all the functions $g(r)$ and $y(r)$ in Fig.

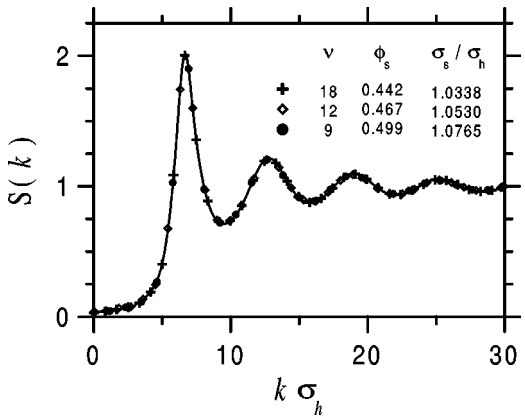

FIG. 2. Structure factor of three equivalent systems of soft spheres. The solid curve corresponds to the system of hard spheres with volume fraction of 0.4.

1 are plotted as functions of the radial distance measured with a common length scale, for which we chose the hard-sphere diameter σ_h. In the figure, we also indicate the value of the soft-sphere diameter σ_s, and the corresponding volume fraction $\phi_s \equiv \pi n \sigma_s^3/6$, for each soft-sphere system (i.e., each value of ν). Since all the systems are supposed to have the same number concentration n, it is not difficult to see that, for a given ν, the volume fractions ϕ_h and ϕ_s are related by $\phi_h/\phi_s = (\sigma_h/\sigma_s)^3$. In determining the value of σ_s that matches the structure of the HS system, one may start with one of the simple prescriptions referred to above, such as the blip function method, but at high concentrations a more accurate prescription may be necessary (see Sec. IV below).

Clearly, this ''structural identity'' refers to the position and height of the successive maxima and minima of $g(r)$, *and not to the details of its main peak at contact.* However, many other properties, including the dynamic properties we are interested in, happen to be quite insensitive to the details of the differences in the rdfs illustrated in Fig. 1. For example, the same differences are virtually indistinguishable when the information in Fig. 1 is presented in the Fourier space, as is illustrated in Fig. 2, where we plot the static structure factor $S(k) = 1 + nh(k)$, where $h(k)$ is the Fourier transform of the total correlation function $h(r) = g(r) - 1$. This figure clearly indicates that, as far as the static structure factor is concerned, there is little difference, within the resolution of the figure, between the hard-sphere and the various soft-sphere systems. A situation similar to this will be found to apply for the dynamic properties of interest, as we explain in the following section.

To avoid confusion, we should stress that the structural equivalence illustrated in Fig. 1 refers to the comparison of the radial distribution functions of several soft-sphere systems which only have in common the value of the number concentration n, but not the value of the volume fraction $\phi_s = \pi n \sigma_s^3/6$. This is because the soft-sphere diameter of each system was adjusted precisely to satisfy the condition for equivalence [see Eq. (5) below], which leads to the coincidence illustrated in the figure. In contrast, one could also compare the rdfs of several soft-sphere systems at the same number concentration and the same soft-sphere diameter (and, hence, the same volume fraction). These systems, however, will not be structurally equivalent, except in the limit of infinitely steep potentials. Comparisons of this sort, not only for structural but also for dynamic and transport properties, have been performed by several authors, most notably by Heyes and co-workers [21–23] (see, for example, Fig. 1 of Ref. [21]).

III. DYNAMIC EQUIVALENCE BETWEEN SOFT- AND HARD-SPHERE SYSTEMS

One of the most directly measurable dynamic phenomena of a colloidal dispersion is the relaxation of the fluctuations $\delta n(\mathbf{r},t)$ of the local concentration $n(\mathbf{r},t)$ of colloidal particles around its bulk equilibrium value n. The average decay of $\delta n(\mathbf{r},t)$ is described [1,2] by the time-dependent correlation function $\langle \delta n(\mathbf{r},t)\, \delta n(\mathbf{r}',0) \rangle$, referred to as the Van Hove function $G(|\mathbf{r}-\mathbf{r}'|,t)$. These properties can be determined directly by means of techniques such as digital video microscopy. Dynamic light scattering, on the other hand, measures directly the Fourier transform $F(k,t)$ of $G(r,t)$, referred to as the intermediate scattering function. These properties contain, in principle, all the relevant dynamic information of the equilibrium suspension. The initial values of these time-dependent correlation functions are precisely the static properties discussed in the preceding section. Thus, we have that $G(r,t=0) = \delta(r) + g(r)$, whereas $F(k,t=0) = S(k)$. The microscopic definition of $G(r,t)$ is the following:

$$G(|\mathbf{r}-\mathbf{r}'|,t) = \frac{1}{N} \left\langle \sum_{i,j=1}^{N} \delta(\mathbf{r}-\mathbf{r}_i(t)) \delta(\mathbf{r}'-\mathbf{r}_j(0)) \right\rangle. \quad (2)$$

In this equation, the angular brackets indicate equilibrium ensemble average. Thus, $G(r,t)$ can be separated into its self and distinct parts $G_s(r,t)$ and $G_d(r,t)$, defined, respectively, as the sum of the diagonal and of the off-diagonal terms of Eq. (2). Clearly, the initial value of $G_s(r,t)$ is $\delta(r)$, and that of $G_d(r,t)$ is $g(r)$.

We can now state the expected dynamic equivalence between soft- and hard-sphere systems in terms of $G(r,t)$. This is basically as simple as the static equivalence explained in the preceding section. Thus, we expect that the Van Hove function of all the systems in Fig. 1, when evaluated at a given nonzero value of the correlation time t, will coincide among themselves, just as they coincide at $t=0$ in Fig. 1.

This expectation, however, involves an additional requirement of dynamic character, namely, that the microscopic dynamic laws that govern the motion of the set of N particles are the same for all the systems we are comparing. By this we mean, in the context of colloid dynamics, that the motion of the N particles of any of these systems is governed, for example, by the N-particle Smoluchowski equations without hydrodynamic interactions (or the equivalent many-particle configurational Langevin equations [2,3]). The practical implementation of the solution of this many-particle dynamic description in a computer simulation corresponds to the well-known Brownian dynamics algorithm of Ermak and McCammon [4]. In the absence of hydrodynamic interactions,

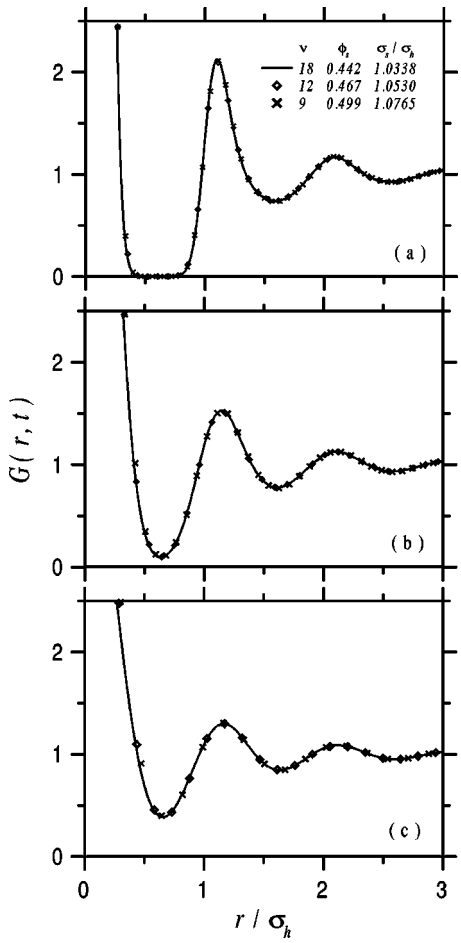

FIG. 3. Van Hove function of three equivalent systems of soft spheres evaluated at three times, namely, $D^0t/\sigma_h^2=0.009$ (a), 0.044 (b), and 0.088 (c). These three systems are equivalent to the system of hard spheres with volume fraction of 0.4.

the only microscopic parameter of dynamic significance in this algorithm is the diffusion coefficient D^0, which governs the free diffusion of each particle, i.e., its motion between collisions. Thus, the Van Hove Function, and all the other macroscopic dynamic properties that derive from it, can only depend on D^0, pair potential and concentration. As in Fig. 1, we are considering the various soft-sphere systems to be at the same number concentration, and we now also assume that each particle diffuses between collisions with the same diffusion coefficient D^0. Thus, our expectation is that, under these assumptions, the details of the interparticle collisions, which are governed by the specific pair potential, will be essentially irrelevant.

In Fig. 3, we plot the Brownian dynamics results for the Van Hove function of the same soft-sphere systems as in Fig. 1, as a function of the radial distance, also expressed in units of σ_h, and for three values of the correlation time t, expressed in terms of a common time unit, for which we choose $\tau_h \equiv \sigma_h^2/D^0$. This figure demonstrates the dynamic equivalence between the three soft-sphere systems simulated with the BD algorithm. Clearly, the quantitative coincidence is much more striking, compared with that observed at $t=0$ in Fig. 1. The reason for this is that the Brownian motion of the particles almost immediately blurs the details of the initial structure represented by $g(r)$, whose first maximum exhibits rather dramatically the detailed differences originating from the difference in the softness of the three systems considered. The curve, in which the three simulation results in Fig. 1 collapse, then represents a universal curve for all the systems in the family in Eq. (1), including the hard-sphere limit $\nu\rightarrow\infty$ (see, however, the limitations discussed in Sec. V). Figure 3 is aimed at illustrating the dynamic extension of the structural equivalence among soft, but short-ranged repulsive potentials of the type in Eq. (1). Exactly the same scenario illustrated in Fig. 3 for $\phi_h=0.4$ was observed for other representative values of ϕ_s in the fluid regime $0 \leqslant \phi_s \leqslant 0.5$. Furthermore, as we said in the beginning of this section, this equivalence is not restricted to the systems whose pair potential is given by the particular functional form in Eq. (1). Although we do not report in detail, similar comparisons as in Figs. 1–3 were made for other functional forms, leading to the same scenario.

We must admit that the dynamic equivalence explained in this section is a rather obvious and naturally expected concept. In fact, the reported experimental measurement of the properties of real hard-sphere dispersions [24–26] is necessarily based on the validity of this equivalence, since real dispersions are never strictly hard spheres. In reality, the measurements are made on soft-sphere dispersions, and it is only on the basis of the equivalence illustrated here in detail, that such measurements can be reported as the properties of hard-sphere systems (see, for example, Refs. [24–26], and references therein). Thus, the value of the results in this section is that they document in detail the degree to which this expectation is correct. Equally important, however, is the fact that this equivalence provides us with a relatively simple method to simulate the properties of an important reference system, namely, the hard-sphere dispersion in the absence of hydrodynamic interactions.

IV. BROWNIAN DYNAMICS ALGORITHM FOR HARD SPHERES

The comparison in Fig. 3 illustrates the notion that it is possible to map the dynamic properties of the hard-sphere Brownian fluid (HSBF) onto the corresponding properties of a soft-sphere system. This correspondence can be stated as follows. Imagine we wish to calculate the Van Hove function $G^H(r,t;n,\sigma_h,D^0)$ of the HSBF for a given state, i.e., for a given volume fraction. Imagine, on the other hand, that one can determine the Van Hove function $G^S(r,t;n,\sigma_s,D^0)$ of a soft-sphere Brownian fluid of arbitrary diameter σ_s, diffusion constant D^0, and concentration n. The equivalence principle that we aim at describing, and that was illustrated in advance in Fig. 3, can then be stated by saying that it is possible to find a value of the soft-sphere diameter σ_s, such that the Van Hove function of both systems are indistinguishable (up to the degree explained in the static case), i.e.,

$$G^H(r,t;n,\sigma_h,D^0)=G^S(r,t;n,\sigma_s,D^0), \tag{3}$$

provided that both systems have the same number concentration n, the same free-diffusion coefficient D^0, and that their

TABLE I. Parameters of the soft-sphere systems calculated with the equivalence approach described in Sec. II. The parameter ν is the exponent in the potential, σ_s is the diameter, and ϕ_s is the volume fraction of soft-sphere system. The last column corresponds to the volume fraction ϕ_h of the equivalent hard-sphere system.

ν	σ_s/σ_h	ϕ_s	ϕ_h
18	1.0344	0.5534	0.5000
12	1.0523	0.5827	0.5000
9	1.0705	0.6133	0.5000
18	1.0344	0.5146	0.4650
18	1.0338	0.4420	0.4000
12	1.0530	0.4670	0.4000
9	1.0765	0.4990	0.4000
18	1.0378	0.3800	0.3400
18	1.0370	0.2230	0.2000

diameters σ_h and σ_s satisfy the condition that the two systems are structurally identical, in the sense explained in the preceding section.

This general dynamic equivalence condition can also be written in terms of the ''natural'' dimensionless variables of each system, as the following rescaling prescription. The Van Hove function of the HSBF can be written in terms of its natural dimensionless arguments as $G^H(r,t;n,\sigma_h,D^0) = G^{H*}(r/\sigma_h,\sigma_h^2 t/D^0;n\sigma_h^3) \equiv G^{H*}(r^*,t^*;n^*)$. Similarly, the Van Hove function $G(r,t)$ of the soft-sphere system depends on the parameters n, σ_s, and D^0 as $G^S(r,t;n,\sigma_h,D^0) = G^{S*}(r/\sigma_s,\sigma_s^2 t/D^0;n\sigma_s^3)$. Thus, the dynamic equivalence condition in Eq. (3) can also be written as

$$G^{H*}(r^*,t^*;n^*) = G^{S*}(\lambda^{-1}r^*,\lambda^2 t^*;\lambda^3 n^*), \tag{4}$$

where $\lambda \equiv \sigma_s/\sigma_h$ is determined by the condition of static structural equivalence, i.e., as the solution of Eq. (4) with $t^*=0$. Since at this initial time the Van Hove function is just the radial distribution function $g(r)$ (for $r \neq 0$), such a condition of static structural equivalence reads

$$g^{H*}(r^*;n^*) = g^{S*}(\lambda^{-1}r^*;\lambda^3 n^*), \tag{5}$$

where the respective rdfs are expressed in terms of the corresponding dimensionless arguments. Equation (5) is the basic assumption on which the specific and approximate prescriptions involved in the WCA and BH perturbation theories are based [1]. For example, integrating this equation is equivalent to the request that the static structure factor at zero wave vector (i.e., the isothermal compressibility) of both systems be the same. The resulting equation is a closed equation for λ, from which even simpler approximate conditions can be derived; the so-called blip-function equation is about the simplest and most elegant (but not sufficiently accurate) of them.

TABLE II. Parameters of the different Brownian dynamic simulations of the soft-sphere systems. The last three columns correspond to the value of the time step Δt, the number of particles $N = 6\phi(L/\sigma_s)^3/\pi$, with $L \approx 7\sigma_s$, and the total number N_c of generated configurations, respectively.

ν	ϕ_s	$D^0\Delta t/\sigma_s^2(\times 10^{-5})$	N	$N_c(\times 10^3)$
18	0.5534	1.64	363	510
12	0.5827	1.64	382	510
9	0.6133	1.73	402	600
18	0.4420	1.63	290	510
12	0.4670	1.64	306	510
9	0.4990	1.53	327	510
18	0.2230	1.48	147	1650

Thus, the first step in the algorithm to simulate the dynamic properties of the HSBF for a given volume fraction $\phi_h = \pi n \sigma_h^3/6$ starts with the determination of λ from some criterion equivalent to Eq. (5). In practice, we first estimate λ (for a given ν) by means of the blip-function method, but then fine tune the determination of λ by performing various simulation runs for the radial distribution function of the soft-sphere system, varying the volume fraction $\phi_s = \lambda^3 \phi_h$, until the integrated form of Eq. (5) is satisfied. Table I contains the values of λ for the soft-sphere potentials and concentrations considered in this paper. In addition, in Table I, we also include two volume fractions corresponding to reported experimental conditions [24,25]. From this table, one can see that, to a first approximation, this quantity is fairly independent of volume fraction, and not very different from the value given by the blip-function method.

Once λ has been determined, the next step is to perform a conventional Brownian dynamics simulation of the soft-sphere system for the resulting volume fraction ϕ_s, following the well-established Ermack-McCammon BD algorithm. The desired data for the HSBF are then given by the simulated properties of the soft-sphere system according to the rescaling prescription in Eq. (4). In Table II, we summarize the technical data of some of the runs whose results are reported in this paper. In particular, the data presented in Fig. 3 to illustrate the dynamic equivalence condition were obtained by following the procedure above.

V. ILLUSTRATIVE APPLICATION

In what follows, we present a selection of representative results for the dynamics of the HS system simulated with the algorithm above. The idea is only to give some details of the methodological procedure, rather than reporting or analyzing the many new data that can be generated as a result of its application, which will be the subject of a separate report [27]. The Van Hove function $G(r,t)$ is the most fundamental dynamic property of a fluid in the equilibrium state, and other properties (such as the self-diffusion and the rheological properties) derive from it. Clearly, properties that can be written only in terms of $G(r,t)$ will inherit the scaling fea-

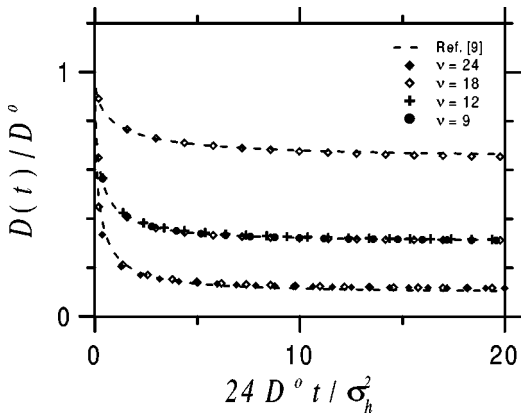

FIG. 4. Time-dependent self-diffusion coefficient of different soft-sphere systems equivalent to the hard-sphere system with volume fraction 0.2 (top), 0.4 (center), and 0.5 (bottom). The dashed curve corresponds to the parametrized fit of the hard-sphere Brownian dynamics reported in Ref. [8].

tures implied by the dynamic universality (or equivalence) principle discussed in this work and illustrated in Fig. 3 for $G(r,t)$ itself. This figure illustrates the general level of quantitative accuracy of these scaling features in $G(r,t)$ at the relevant space- and time-regimes. One can intentionally search, however, for properties that exhibit more dramatically the deviations from this scaling behavior. One of them is, of course, $G_d(r,t)$ near $r=\sigma_h$ at very early times, since $G_d(r,t=0)=g(r)$, which strongly depends on ν near $r=\sigma_h$ (see Figs. 1 and 5 below).

Another sensitive property is the mean squared displacement of individual particles. For example, in Fig. 4, we present results for the dimensionless time-dependent self-diffusion coefficient $D(t)/D^0$ of the soft-sphere systems with $\nu=9,12,18,24$ at the HS volume fractions of 0.2, 0.4, and 0.5. This property is defined [2,3] as the mean squared displacement of a tracer particle divided by its free-diffusion limit $6D^0t$, so that $D(t)/D^0 \equiv \langle [\Delta r(t)]^2 \rangle / 6D^0 t$. Clearly, the curves corresponding to the soft-sphere systems with $\nu=9$, 12, and 18 collapse into a single curve. This curve will then be the same for the other soft-sphere systems in the family (i.e., for all other values of ν), and hence, it will also represent the properties of the hard-sphere system. With this confidence, in Fig. 4, we only plot the specific results obtained with the system $\nu=18$ for the lowest volume fraction ($\phi_h=0.2$).

The range of validity of the above method depends, however, on various factors. For example, the soft-sphere systems included in the equivalence family cannot, of course, be arbitrarily soft, i.e., ν cannot be close to, for example, 1 or 2. Typical values of ν for which our scheme applies with confidence are those reported in our illustrative examples ($\nu=9,12,18$). We found, however, that at volume fractions of the order of, and beyond, the freezing volume fraction ϕ_f, the softer of these systems, in spite of being structurally equivalent, may fall outside the range of dynamical equivalence. This is also illustrated in Fig. 4, by the average of $D(t)$ corresponding to various soft-sphere systems ($\nu=9$, 12, 18, and 24) which are structurally identical to the HS system at the volume fraction of 0.5. Clearly, now there is a slight but appreciable dependence on ν of the results for $D(t)/D^0$ for the softer potentials ($\nu=9$ and 12), and one has to go beyond $\nu=18$ in order to see the convergence into a single curve, corresponding to the hard-sphere system. This is illustrated with the data for $\nu=24$, which already fall inside the universal curve for this volume fraction, and hence, represent a very accurate determination of the time-dependent properties of the HS system.

Thus, our procedure has its own self-consistency criterion to estimate the accuracy to which we are determining the dynamic properties of the HS system, namely, the collapse of the results of all soft-sphere systems (beyond some threshold value of ν, which may depend on volume fraction) into a single curve. Nevertheless, it is reassuring to check that our results coincide with those determined by means of different and independent approaches. In this respect, we found that our data agree with those of Cichocki and Hinsen, represented in Fig. 4 by the dashed curves, which derive from the parametrized formula that these authors used to fit their simulation data in Ref. [8].

Another regime where our equivalence principle must require careful application refers to short times. All we have said so far is based on the results plotted in our illustrative figures. They correspond to a time window with a time scale $\tau_0 \equiv \sigma_h^2/D^0$, which is the time needed by a given particle to diffuse its own HS diameter. This, however, may be a rather long time compared with the mean time this particle takes to diffuse freely, before colliding with other spheres. A simple estimate of this mean free time τ_f is given by the time one particle takes to diffuse the surface-to-surface mean distance $(d-\sigma_h)$, where $d=n^{-1/3}$ is the interparticle mean distance, i.e., $\tau_f \equiv (d-\sigma_h)^2/D^0$. Thus, the ratio $\tau_f/\tau_0=(d/\sigma_h-1)^2$ depends on concentration. For a packing fraction of 0.4, this ratio is of the order of 10^{-2}. This means, for example, that the results illustrated in Fig. 3, which correspond to times $t/\tau_0 \geqslant 0.875\times 10^{-2}$, illustrate only the collision-dominated regime. In order to observe the free-diffusion regime, $t \lesssim \tau_f$, we would have to increase the time resolution by at least one order of magnitude. If this is done, one would observe how the initial structure, determined by the radial distribution function $g(r)$, is dissipated only by the free diffusion of the particles that constitute the cage around the central particle. Since, as we see in Fig. 1, the differences between the various soft-sphere systems are most apparent in the first maximum of $g(r)$, one can expect that in this very early time regime such differences should still be apparent in the distinct part $G_d(r,t)$ of the Van Hove function. To provide a more quantitative illustration of this, Fig. 5 describes the evolution of the first maximum of $G_d(r,t)$ for three times pertaining to this short-time regime. Let us mention, however, that these differences between different systems only become an issue when we observe them in $G_d(r,t)$ or in the full Van Hove function in this early time regime. However, if the same information were presented in the Fourier space, we would hardly be able to appreciate them, since these differences are negligible already for the static structure factor, as illustrated in Fig. 2.

Concerning the results for the time-dependent diffusion

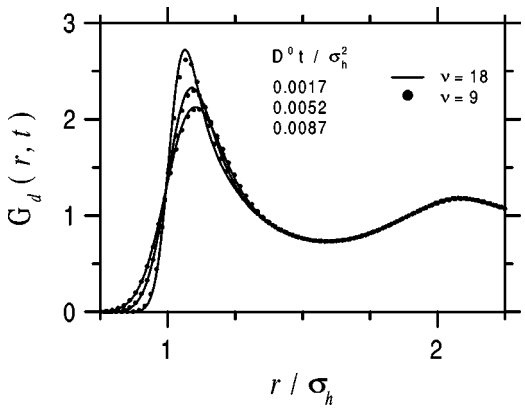

FIG. 5. Distinct part of the Van Hove function of two equivalent systems of soft-spheres evaluated at three different times in the short-time regime. Both systems are equivalent to the hard-sphere system at volume fraction 0.4.

coefficient in Fig. 4, the free-diffusion regime corresponds to the very initial decay of $D(t)/D^0$ from its value of 1 at $t=0$. In this figure, this decay is hidden in the almost vertical decay of $D(t)/D^0$. If we again look at this time regime with much higher resolution, we would again notice differences (particularly in the initial slope of this quantity) for different soft-sphere systems. In fact, it is not difficult to show that the value of this initial slope is proportional to ν^{-1}, and hence, it diverges for the hard-sphere system. However, as soon as the collisions dominate the structural relaxation, i.e., for times larger than τ_f, these initial differences become irrelevant, as demonstrated here.

From the experimental point of view, the relaxation of the fluctuations in the Fourier space constitutes a more relevant subject. Only as an illustration, in Fig. 6, we present the decay of the intermediate scattering function $F(k,t)$ for the hard-sphere system at a packing fraction of 0.50 and at the wave vector $k_{\min}$ corresponding to the position of the minimum of the static structure factor. This figure complements Fig. 4 in the comparison of our simulation results with those

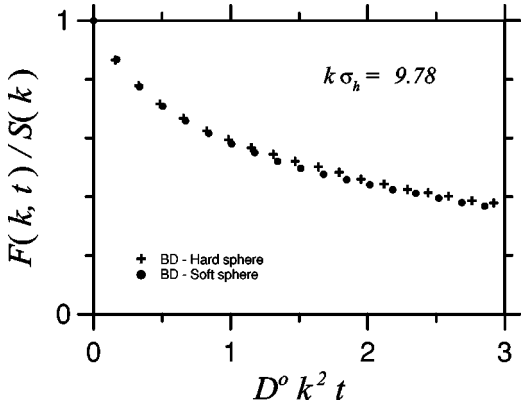

FIG. 6. Intermediate scattering function of the system of soft spheres with volume fraction of 0.5534 and exponent $\nu=18$, equivalent to the hard-sphere system at volume fraction 0.50. The wave vector $k\sigma_h=9.78$ corresponds to the position of the first minimum of the static structure factor $S(k)$.

of the alternative method of Cichocki and Hinsen. Here again, we find total agreement between the results of the two methods.

VI. SUMMARY

In this paper, we have demonstrated that the principle of static structural equivalence among systems with purely repulsive interactions carries over to the dynamic domain. The results presented here indicate the degree to which this principle applies in the realm of the collective dynamic properties, such as the Van Hove function, of model Brownian fluids. We demonstrated that this principle applies to such a degree of quantitative accuracy, that it lends itself to a practical application, namely, the devise of a simple algorithm to carry out Brownian dynamics simulations of the properties of an important reference system, namely, the hard-sphere Brownian fluid in the absence of hydrodynamic interactions. Here, we also provided detailed explanation of a number of methodological issues of the application of this simulation algorithm. This algorithm has its own internal criterion of reliability, namely, the collapse of the results for a given dynamic property for different soft-sphere systems in a single master curve. However, it was interesting to establish that the results of our algorithm agree with the available results of the method of Cichocki and Hinsen [8–11].

Although in practice this may not be quantitatively very relevant, here we also discussed the range of validity of our proposal. Thus, the principle of dynamic correspondence has the same limitations as its static version, namely, the structural equivalence does not refer to the region near contact, where the details of the specific interaction potential matter. In the dynamic version, however, these details only remain appreciable at very early times, and are quickly and completely blurred out as soon as the interparticle collisions become important. A more important and fundamental potential limitation refers to the application of these ideas to nonequilibrium conditions [15]. Our interest in developing this method of simulating the dynamics of the equilibrium HSBF, however, derives from the need of understanding important issues involving this relevant reference system. For example, given a number of interesting observations on the dynamic properties of experimental HS colloidal systems [24–26], it would be interesting to see which of these observations are a consequence only of the direct interactions, and which of them derive fundamentally from the presence of hydrodynamic interactions in a real suspensions. The complexity of the theoretical treatment of the combined effects of hydrodynamic and direct interactions in highly concentrated dispersions call for simplifying approaches to the description of these phenomena, such as the hydrodynamic rescaling concept put forward in 1988 by one of the authors [28]. In these efforts, and in the devise and calibration of approximate theoretical schemes [29], one might benefit from the availability of a variety of manners to simulate the properties that these theories predict. As it happens, the simulation algorithm pre-

sented in this paper turns out to be an effective tool for the purposes just mentioned, as reported separately [27].

ACKNOWLEDGMENTS

This work was supported by the Instituto Mexicano del Petróleo, through Grant No. FIES-98-101-1, and by the Consejo Nacional de Ciencia y Tecnolog ía (CONACYT, México), through Grant Nos. G295589-E and NC0072: Materiales Biomoleculares. M.M.N. acknowledges the kind hospitality of the Departamento de Física del Centro de Investigación y de Estudios Avanzados del Instituto Politécnico Nacional (CINVESTAV-IPN, México city).

[1] J.P. Hansen and I.R. McDonald, *Theory of Simple Liquid* (Academic Press, New York, 1986).
[2] P.N. Pusey, *Liquids, Freezing and the Glass Transition* (Elsevier, Amsterdam, 1991).
[3] G. Nägele, Phys. Rep. **272**, 215 (1996).
[4] D.L. Ermak and J.A. McCammon, J. Chem. Phys. **69**, 1352 (1978).
[5] M.P. Allen and D.J. Tildesley, *Computer Simulation of Liquids* (Clarendon Press, New York, 1987).
[6] P. Strating, Phys. Rev. E **59**, 2175 (1999).
[7] Y. Terada and M. Tokuyama, J. Korean Phys. Soc. **38**, 512 (2001).
[8] B. Cichocki and K. Hinsen, Ber. Bunsenges. Phys. Chem. **94**, 243 (1990).
[9] B. Cichocki and K. Hinsen, Physica A **166**, 473 (1990).
[10] B. Cichocki and K. Hinsen, Physica A **187**, 133 (1992).
[11] B. Cichocki and B.U. Felderhof, Physica A **204**, 152 (1994).
[12] D.M. Heyes and J.R. Melrose, J. Non-Newtonian Fluid Mech. **46**, 1 (1993).
[13] W. Shaertl and H. Sillescu, J. Stat. Phys. **74**, 687 (1994).
[14] W. Shaertl and H. Sillescu, J. Stat. Phys. **79**, 299 (1995).
[15] D.R. Foss and J.F. Brady, J. Rheol. **44**, 629 (2000).
[16] D.M. Heyes and A.C. Brańka, Phys. Rev. E **50**, 2377 (1994).
[17] D.M. Heyes, Mol. Phys. **87**, 287 (1996).
[18] H.C. Andersen, J.D. Weeks, and W. Chandler, Phys. Rev. A **4**, 1597 (1971).
[19] J.D. Weeks, W. Chandler, and H.C. Andersen, J. Chem. Phys. **54**, 5237 (1971).
[20] J.A. Barker and D. Henderson, J. Chem. Phys. **47**, 4714 (1967).
[21] D.M. Heyes, J. Phys.: Condens. Matter **6**, 6409 (1994).
[22] D.M. Heyes and J.G. Powles, Mol. Phys. **95**, 259 (1998).
[23] J.G. Powles *et al.*, Proc. R. Soc. London, Ser. A **455**, 3725 (1999).
[24] P.N. Segrè and P.N. Pusey, Phys. Rev. Lett. **77**, 771 (1996).
[25] L.B. Lurio *et al.*, Phys. Rev. Lett. **84**, 785 (2000).
[26] D. Lumma *et al.*, Phys. Rev. E **62**, 8258 (2000).
[27] F. Guevara-Rodríguez *et al.* (unpublished).
[28] M. Medina-Noyola, Phys. Rev. Lett. **60**, 2705 (1988).
[29] L. Yeomans-Reyna *et al.*, Phys. Rev. E **67**, 021108 (2003).